

Anisotropic Log-Gaussian Cox Processes Using Normal Variance Mixture Covariance Function

Fariba Nasirzadeh^{1*}, Zohreh Shishebor¹, Jorge Mateu²

¹ Department of Statistics, Faculty of Science, Shiraz University, Shiraz, Iran.

² Department of Mathematics, University Jaume I, Castellon, Spain

Abstract:

In this paper, we introduce a new family of anisotropic log Gaussian Cox processes (LGCPs) that is useful to model spatial anisotropic point patterns that depict a degree of clustering. Our idea lies in building a new family of anisotropic LGCP using the normal variance mixture covariance function. We describe the moment properties of our new model. Finally, the estimation procedure is evaluated through a simulation study.

Keywords: Anisotropy, Clustering, Covariance function, K -function, Log Gaussian Cox processes, Normal variance mixture.

Mathematics Subject Classification (2010): 74E10, 91C20, 60G55.

1 Introduction

A Cox process is a natural extension of a Poisson process, obtained by considering the intensity function of the Poisson process as a realization of a random field (Cox, 1955).

One specific forms of the Cox process are the class of LGCPs. The class of LGCPs has been introduced in astronomy by Coles and Jones (1991) and in statistics by Møller and *et al.* (1998). The LGCP construction has an elegant simplicity. One is that the tractability of the multivariate normal distribution carries over, to some extent, to the associated Cox process. LGCPs from different aspects are studied in many papers such as Diggle and *et al.* (2013), Siino and *et al.* (2018) and Teng and *et al.* (2017).

Under ergodicity, a point process is stationary and isotropic, if its statistical properties do not change under translation and rotation, respectively. However, this assumption is

*Speaker: nasirzadeh_fariba@yahoo.com

not realistic and it is not satisfied in many real applications. A spatial point pattern is called anisotropic if its spatial structure depends on the direction. Redenbach and *et al.* (2009), Møller and Rasmussen (2012), Møller and Toftaker (2014), Fuglstad and *et al.* (2013), Allard and *et al.* (2016), and Comas and *et al.* (2018) studied an anisotropic models that are more focused on testing anisotropy and describing main directions.

Here, we are interested in point pattern models for anisotropic behaviors, and in this sense the literature is scarce. In particular, we develop a new class of anisotropic LGCPs while finding analytical form for the covariance of the associated random field. Our idea lies in building an anisotropic covariance function. The prerequisites for LGCPs are explained in Section 2. In Section 3, we describe the normal variance mixture covariance functions. A new family of anisotropic LGCP using an anisotropic normal variance mixture covariance function is presented in Section 4. The method of parameter estimation is described in Section 5. Finally, we present a simulation study to evaluate our presented model.

2 Prerequisites

A spatial point process X is considered as a random countable subset of a space S , where $S \subseteq \mathbb{R}^d$. The first-order properties of point process X are called intensity function and shown by $\lambda(x)$. If λ is constant, then X is said to be homogeneous or first-order stationary with intensity λ ; otherwise, X is said to be inhomogeneous. For a homogeneous point process, λ is the mean number of points per unit volume and the constant is called intensity or rate.

Suppose that $\Lambda = \{\Lambda(x) : x \in S\}$ is a non-negative random field so that with probability one, $x \rightarrow \Lambda(x)$ is a locally integrable function. If the conditional distribution of X given the realization $\Lambda(x) = \lambda(x)$ is an inhomogeneous Poisson process on S with intensity function $\lambda(x)$, then X is said to be a Cox process driven by Λ . One specific and flexible forms of Cox processes are LGCPs that have been introduced in astronomy by Coles and Jones (1991) and in statistics by Møller and *et al.* (1998). As the name implies, an LGCP is a Cox process with $\Lambda(x) = \exp\{Z(x)\}$, where Z is a Gaussian process.

By stationarity, the distribution of $Z(x)$ and hence X is specified by the mean, $\mu_Z = \mathbb{E}[Z(x)]$, the variance $\sigma_Z^2 = \text{Var}[Z(x)]$, the correlation function $r_Z(u)$, and the covariance function $C_Z(u) = \sigma_Z^2 r_Z(u)$ of Z . The model is only well-defined for positive semi-definite correlation functions, i.e. when $\sum_{i,j} a_i a_j r(x_i - x_j) \geq 0$ for all $a_1, a_2, \dots, a_n \in \mathbb{R}$, $x_1, x_2, \dots, x_n \in \mathbb{R}$, $n = 1, 2, \dots$

The first- and second-order moment properties of LGCP X is given in Table 1.

If the PCF exists and is invariant under translations, then we have second-order intensity

Table 1: The moment properties of LGCPs driven by intensity function $\Lambda(x) = \exp\{Z(x)\}$.

Moment properties	Formula
Intensity function	$\lambda = \exp\{\mu_Z + \frac{1}{2}\sigma_Z^2\}$
Second-order intensity function	$\mathbb{E}[\Lambda(x)\Lambda(x-u)] = \exp\{2\mu_Z + \sigma_Z^2\} [1 + r_Z(u)]$
Covariance density function	$\gamma(u) = \exp\{2\mu_Z + \sigma_Z^2\} [\exp\{C_Z(u)\} - 1]$
Pair Correlation Function (PCF)	$g(u) = 1 + \frac{\gamma(u)}{\lambda^2} = \exp\{C_Z(u)\}$

reweighted stationarity and a close relationship between the κ -measure and the PCF as

$$\kappa(B) = \int_B g(u) du, \quad B \subseteq \mathbb{R}^d, \quad (2.1)$$

where u is the separation vector. For more details, refer to [Illian and *et al.* \(2008\)](#).

3 Normal variance mixture covariance model

3.1 Normal variance mixture function

[Jalilian and Waagepetersen \(2013\)](#) introduced a new class of isotropic shot noise Cox processes in which both the kernel function and the PCF are given based on a normal variance mixture. Modeling the shape at the origin and the tail behavior of the PCF can be easier and more flexible when using the normal variance mixture. We now follow this method to obtain an anisotropic covariance function and then a new anisotropic class of LGCPs. The normal variance mixture density function is defined by

$$f(u) = \int_0^\infty \Phi(u; s) h(s) ds, \quad (3.1)$$

where $\Phi(\cdot; s)$ is the density of a zero-mean two-dimensional anisotropic Gaussian vector with covariance matrix sM , $M = \text{diag}(\sigma_1, \sigma_2)$, and h is some prior probability density of s on \mathbb{R}^+ . Any function f defined as in (3.1) is a positive definite function on \mathbb{R}^2 ([Schlather, 1999](#)). By a similar argument to the isotropic case, if h is a convolution of a function \tilde{h} with itself, i.e. $h = \tilde{h} * \tilde{h}$, then f is the convolution of a non-negative function k with itself, $f = k * k$, where the function k is defined by

$$k(u) = \int_0^\infty \Phi(u; s) \tilde{h}(s) ds. \quad (3.2)$$

According to the relation between Equations (3.1) and (3.2), f can be considered as a covariance function. We discuss below a special case of \tilde{h} and obtain the Cauchy covariance function. The Cauchy covariance function is polynomially decreasing, and hence more

suitable than the Matérn model for modeling slowly decaying covariances. The Cauchy covariance is log-concave in a neighborhood around the origin.

3.2 Anisotropic Cauchy covariance model

Assume that s in Equation (3.2) is a random variable with an inverse Gamma density with parameters $\alpha, \beta > 0$ of the form $h(s; \alpha, \beta) = \beta^\alpha s^{-\alpha-1} \exp\{-\beta/s\} / \Gamma(\alpha)$, $s > 0$. Let $\alpha = 1/2$. It can be shown that $h(\cdot; 1/2, \beta)$ is a convolution of $h(\cdot; 1/2, \beta/4)$ with itself. Following Equations (3.1) and (3.2), a covariance function can be defined through a normal variance mixture with the function $h(\cdot; 1/2, \beta)$, as follows

$$\begin{aligned} C_{aniso}(u) &= \int_0^\infty \frac{1}{2\pi s \sqrt{\sigma_1 \sigma_2}} \exp\left\{-\frac{u_1^2}{2\sigma_1 s} - \frac{u_2^2}{2\sigma_2 s}\right\} \frac{\beta^{\frac{1}{2}}}{\Gamma\left(\frac{1}{2}\right)} s^{-\frac{3}{2}} \exp\{-\beta/s\} ds \\ &= \frac{1}{4\pi\beta\sqrt{\sigma_1\sigma_2}} \left[1 + \frac{u_1^2}{2\sigma_1\beta} + \frac{u_2^2}{2\sigma_2\beta}\right]^{-\frac{3}{2}}, \end{aligned} \quad (3.3)$$

with anisotropic parameters $\sigma_1^* = \sigma_1\beta$, and $\sigma_2^* = \sigma_2\beta$. Equivalently, $C_{aniso}(u) = \sigma^2 [1 + u^T \Sigma^{-1} u]^{-\frac{3}{2}}$ where $\sigma^2 = \frac{1}{4\pi\sqrt{\sigma_1^*\sigma_2^*}}$ is the variance and Σ is an anisotropic diagonal matrix with elements $(2\sigma_1^*, 2\sigma_2^*)$. Clearly, this anisotropic covariance function can be written in terms of the isotropic function, that is, $C_{aniso}(u) = C_{iso}(u^T \Sigma^{-1} u)$ where $C_{iso}(\nu) = \sigma^2 [1 + \nu]^{-\frac{3}{2}}$ is an isotropic Cauchy covariance function (Nasirzadeh and *et al.*, 2021).

4 New family of Anisotropic log Gaussian Cox processes

A LGCP model is driven by a log Gaussian random field. In constructing an anisotropic LGCP model, in terms of the properties of the model, we need a Gaussian random field to have an anisotropic covariance function. In the previous section, we propose a mechanistic procedure based on normal variance mixtures and obtain an anisotropic Cauchy covariance function. Let X be a LGCP with intensity $\Lambda(x) = \exp\{Z(x)\}$ where $Z(\cdot)$ is a Gaussian process with mean μ_Z , variance σ_Z^2 and covariance function $C_Z(\cdot)$ which is defined in Equation (3.3). After the re-parameterization of model as $\Lambda(x) = \exp\{\eta + Z(x)\}$, with $\mathbb{E}[Z(x)] = 0.5\sigma_Z^2$, where σ_Z^2 is the variance of $Z(x)$, we can simply obtain $E[\exp\{Z(x)\}] = 1$ and $\lambda = \exp\{\eta\}$ (Diggle, 2013). As Table 1 and Equation (3.3), the covariance density

function of our model is obtained as

$$\gamma(u) = \exp\{2\eta\} \left[\exp \left\{ \frac{1}{4\pi\sqrt{\sigma_1^*\sigma_2^*}} \left[1 + \frac{u_1^2}{2\sigma_1^*} + \frac{u_2^2}{2\sigma_2^*} \right]^{-\frac{3}{2}} \right\} - 1 \right], \quad (4.1)$$

and the PCF of our model can be obtained as

$$g_{aniso}(u) = \exp \left\{ \frac{1}{4\pi\sqrt{\sigma_1^*\sigma_2^*}} \left[1 + \frac{u_1^2}{2\sigma_1^*} + \frac{u_2^2}{2\sigma_2^*} \right]^{-\frac{3}{2}} \right\} = \exp \left\{ \sigma^2 [1 + u^\tau \Sigma^{-1} u]^{-\frac{3}{2}} \right\}. \quad (4.2)$$

Here, $g_{aniso}(u) = g_{iso}(u^\tau \Sigma^{-1} u)$ where $g_{iso}(\nu) = \exp \left\{ \sigma^2 [1 + \nu]^{-\frac{3}{2}} \right\}$ is an isotropic Cauchy PCF (Nasirzadeh and *et al.*, 2021). For completeness, assume B is a disc centred at the origin with radius ρ , denoted by $d(0, \rho)$ and analytically represented by $\|u\| \leq \rho$. Substituting (4.2) into (2.1), the anisotropic K -function over the disc B , denoted by K_{aniso}^C , is given by $K_{aniso}^C(\rho) = \int_{\|u\| \leq \rho} \exp \left\{ \frac{1}{4\pi\sqrt{\sigma_1^*\sigma_2^*}} \left[1 + \frac{u_1^2}{2\sigma_1^*} + \frac{u_2^2}{2\sigma_2^*} \right]^{-\frac{3}{2}} \right\} du$.

5 Parameter estimation

Let W denotes a bounded window in \mathbb{R}^2 . Suppose that X is a LGCP model defined on W , driven by the random intensity function $\Lambda(x) = \exp \{ \eta + Z(x) \}$, where $Z(x)$ is a Gaussian process with anisotropic Cauchy covariance parameters σ_1 and σ_2 . For parameter estimation, we consider the least squares estimation method that is a moment-based estimation technique based, in our case, on minimizing a measure of the difference between a theoretical K -function and an empirical one. Assume that the model incorporates a vector of unknown parameters θ . Let K_T and K_E denote the theoretical and the empirical K -functions, respectively. A discrepancy criterion to measure the difference between the model, determined by K_T , and empirical data, determined by K_E , is given by

$$D(\theta) = \int_0^{\rho_0} w(\rho) \{K_T(\rho, \theta)^c - K_E(\rho)^c\}^2 d\rho, \quad (5.1)$$

where the constant ρ_0 , the power transformation c , and the weighting function $w(\rho)$ are to be chosen. The value $\hat{\theta}$ obtained by minimizing (5.1) is considered the estimate of the vector of parameters θ . In the general case, as Illian and *et al.* (2008), an inhomogeneous reduced second-moment measure for any bounded set B in \mathbb{R}^2 can be estimated by

$$K_E(\rho) = \sum_{\substack{x_i, x_j \in W \\ x_i \neq x_j}} \frac{I(\|x_j - x_i\| \leq \rho)}{\hat{\lambda}(x_i) \hat{\lambda}(x_j)} e(x_i, x_j), \quad (5.2)$$

where W is a rectangular window, I stands for the indicator function, and $e(x_i, x_j)$ is a weighting function that corrects for edge effects. Also, a non-parametric kernel estimation method is often used to estimate the intensity function of a realization of $X = \{x_i\}_{i=1}^n$, and is given by $\hat{\lambda}(y) = \sum_{i=1}^n k(y - x_i)/e(x_i)$ for any location point y , where $k(y)$ is the kernel function and $e(y) = \int k(y - v)dv$ is an edge correction.

6 Simulation experiment

In this Section, we carried out a simulation study to investigate the performance of our estimation procedure. We assume to work on the unit square, $W = [0, 1] \times [0, 1] \subseteq \mathbb{R}^2$. We first considered 200 realizations from the anisotropic LGCP in Section 4, based on the anisotropic Cauchy covariance function defined in Equation (3.3), with anisotropic parameters given by $\sigma_1 = 0.2$ and $\sigma_2 = 0.045$, and with the scale parameter of the Cauchy covariance $\beta = 1$. Figure 1 (two first columns) represents a simulation of the corresponding underlying random field $Z(\cdot)$ with covariance function given in Equation (3.3), together with the intensity $\Lambda(x) = \exp\{6 + Z(x)\}$ and a realization with 265 points of our presented model.

The simulated data sets should show some sort of anisotropy. For a simple assessment of anisotropy, we follow [Baddeley and et al. \(2015\)](#) that suggested comparing the sector K -function for two 30-degree sectors centered on the x and y axes, i.e., the angle between -15 and 15 degrees and the angle between 90-15 and 90+15 degrees, measured anticlockwise from the x -axis. Anisotropy would be suggested if these two functions were unequal. Figure 1 (two last columns) shows the sector K -functions for 30-degree sectors centered on the horizontal and vertical axis for the particular realization. Anisotropy is clear in this case, for that the two sector K -functions are certainly different.

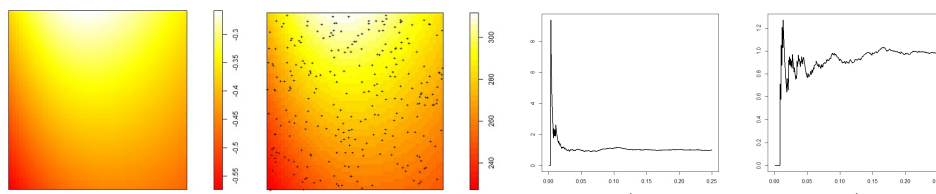


Figure 1: Representations of the random fields (*First column*), and of intensities and point pattern realizations of the presented anisotropic LGCP (*Second column*). Assessment of anisotropy using sector K -functions: sector K -functions for 30-degree sectors centred on the horizontal axis (*Third column*), and sector K -functions for 30-degree sectors centred on the vertical axis (*Fourth column*).

We thus, as an additional assessment, compare the empirical K -function coming from the simulated patterns with the theoretical anisotropic K -function. We also consider

the K -function under a Poisson process over a disc centered at the origin with radius ρ , whose form is $K^{Pois}(\rho) = \pi\rho^2$ (see Figure 3, left). It is noted that our model reflects a clustering behavior as the K -functions are above the Poisson function, and, as expected, the empirical and theoretical K -function behaves in a similar way far from the random case, represented by the Poisson function. This is a direct consequence of the structure imposed by a LGCP with a varying intensity depending on a random field with a particular correlation structure.

Finally, we estimated all parameters of the model for each one of the 200 realizations. The results in form of point estimations, the Mean Absolute Percentage Error (MAPE), Mean Squared Error (MSE), Standard Deviations (SD), and Confidence Intervals (CI) are shown in Table 2. We note that the estimations are close to the true values of the parameters, and the corresponding MAPE, MSE, and SD values are certainly small. Also, the true values of the parameters θ are well inside the 95% confidence intervals, given by $\hat{\theta} \pm 1.96 SD(\hat{\theta})$, where θ stands for any particular parameter (σ_1, σ_2). These results are reinforced by graphical outputs in terms of histograms and boxplots (see Figure 2).

Table 2: Point estimations, MAPE, MSE, SD, and CI of the estimated parameters for the presented LGCP model.

Parameters	Point estimation	MAPE	MSE	SD	CI
$\sigma_1 = 0.2$	$\hat{\sigma}_1 = 0.19979$	0.01797	0.00003	0.0052	(0.19906, 0.20051)
$\sigma_2 = 0.045$	$\hat{\sigma}_2 = 0.04485$	0.03456	0.000004	0.00187	(0.04459, 0.04511)

The true parameters are clearly lying inside the distribution of the estimated parameters. Only in one case, we find a small number of outliers, but even for this case, the difference concerning the mean is so small that they have no particular effect. Also, Figure 3 (Right) shows the theoretical K -function based on the true values of parameters and the theoretical K -functions coming from the estimated values for our model. The theoretical K -function based on the true values are well inside the theoretical K -functions coming from the estimated parameters, which is an indication of robust behavior of the estimation procedure.

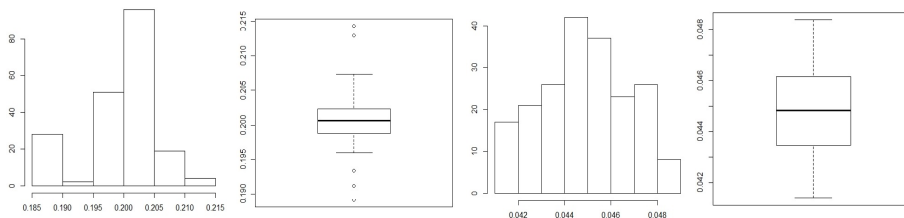


Figure 2: Histograms and boxplots for the estimation of σ_1 (*Two first columns*) and σ_2 (*Two last columns*) using the moment-based estimation method over a disc.

We note that the moment-based estimator based on a moment-based estimation method provides a reasonable performance for mentioned model. The estimation for both parameters are close to the theoretical ones with a small variation. They show some symmetry and there are hardly outlying estimates. The procedure works equally fine for the new theoretical model.

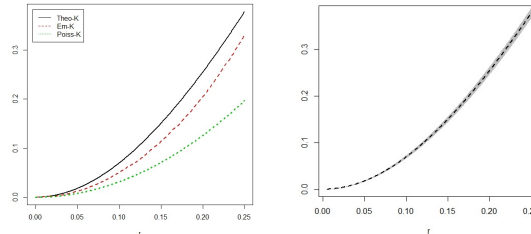


Figure 3: *Left:* Comparison of empirical K -functions (Em-K) with theoretical ones (Theo-K) over a disc for presented anisotropic LGCP, and with the K -function under a PPP (Poiss-K). *Right:* Theoretical K -function based on the true value of parameters (black color) and theoretical K -function based on the point estimations (gray color).

References

- Allard, D., Senoussi, R., and Porcu, E. (2016). Anisotropy models for spatial data. *Mathematical Geosciences*. **48(3)**, 305-328.
- Baddeley, A., Rubak, E. and Turner, R. (2015). *Spatial Point Patterns: Methodology and Applications with R*. CRC Press.
- Coles, P. and Jones, B. (1991). A lognormal model for the cosmological mass distribution. *Monthly Notices of the Royal Astronomical Society*. **248**, 1-13.
- Comas, C., Conde, J. and Mateu, J. (2018). A second-order test to detect spatio-temporal anisotropic effects in point patterns. *Statistics*. **52 (4)**, 717-733.
- Cox, D. R. (1955). Some statistical methods connected with series of events. *Journal of the Royal Statistical Society: Series B (Methodological)*, **17(2)**, 129-157.
- Diggle, P.J. (2013). *Statistical Analysis of Spatial and Spatio-Temporal Point Patterns*. CRC Press.
- Diggle, P.J., Moraga, P., Rowlingson, B. and Taylor, B.M. (2013). Spatial and spatio-temporal log-Gaussian Cox processes: extending the geostatistical paradigm. *Statistical Science*. **28**, 542-563.

- Fuglstad, G. A., Lindgren, F., Simpson, D., and Rue, H. (2015). Exploring a new class of non-stationary spatial Gaussian random fields with varying local anisotropy. *Statistica Sinica*. 115-133.
- Illian, J., Penttinen, A., Stoyan, H. and Stoyan, D. (2008). *Statistical Analysis and Modelling of Spatial Point Patterns*. John Wiley & Sons, 70.
- Jalilian, A., Guan, Y. and Waagepetersen, R. (2013). Decomposition of variance for spatial Cox processes. *Scandinavian Journal of Statistics*. **40**, 119-137.
- Møller, J. and Rasmussen, J.G. (2012). A sequential point process model and bayesian inference for spatial point patterns with linear structures. *Scandinavian Journal of Statistics*. **39**, 618-634.
- Møller, J., Syversveen, A.R. and Waagepetersen, R. (1998). Log Gaussian Cox processes. *Scandinavian Journal of Statistics*. **25**, 451-482.
- Møller, J. and Toftaker, H. (2014). Geometric anisotropic spatial point pattern analysis and Cox processes. *Scandinavian Journal of Statistics*. **41**, 414-435.
- Nasirzadeh, F., Shishebor, Z., and Mateu, J. (2021). On new families of anisotropic spatial log-Gaussian Cox processes. *Stochastic Environmental Research and Risk Assessment*, **35**(2), 185-213.
- Redenbach, C., Sarkka, A., Freitag, J. and Schladitz, K. (2009). Anisotropy analysis of pressed point processes. *Advances in Statistical Analysis*. **93**, 237-261.
- Schlather, M. (1999). *Introduction to positive definite functions and to unconditional simulation of random fields*. Tech. Rep. ST-99-10, Department of Mathematics and Statistics. Faculty of Applied Sciences, Lancaster University, UK.
- Siino, M., Adelfio, G. and Mateu, J. (2018). Joint second-order parameter estimation for spatio-temporal log-Gaussian Cox processes. *Stochastic Environmental Research and Risk Assessment*. **32** (12), 35253539.
- Teng, M., Nathoo, F., and Johnson, T. D. (2017). Bayesian computation for Log-Gaussian Cox processes: A comparative analysis of methods. *Journal of statistical computation and simulation*, **87**(11), 2227-2252.